New Phytologist

Research

Optimal allocation of leaf epidermal area for gas exchange

Hugo J. de Boer[1,2], Charles A. Price[2,3], Friederike Wagner-Cremer[4], Stefan C. Dekker[1], Peter J. Franks[5] and Erik J. Veneklaas[2]

[1]Department of Environmental Sciences, Faculty of Geosciences, Utrecht University, Heidelberglaan 2, 3584 CS, Utrecht, the Netherlands; [2]School of Plant Biology, The University of Western Australia, 35 Stirling Highway, Crawley, WA 6009, Australia; [3]National Institute for Mathematical and Biological Synthesis (NIMBioS), University of Tennessee, 1122 Volunteer Blvd, Suite 106, Knoxville, TN 37996-3410, USA; [4]Department of Physical Geography, Faculty of Geosciences, Utrecht University, Heidelberglaan 2, 3584 CS, Utrecht, the Netherlands; [5]The University of Sydney, Faculty of Agriculture and Environment, Sydney, NSW 2006, Australia

Author for correspondence:
Hugo J. de Boer
Tel: +31 30 2536951
Email: h.j.deboer@uu.nl

Received: *28 December 2015*
Accepted: *8 February 2016*

New Phytologist (2016)
doi: 10.1111/nph.13929

Key words: allometry, evolution, guard cell, leaf gas exchange, leaf morphology, stomata.

Summary

- A long-standing research focus in phytology has been to understand how plants allocate leaf epidermal space to stomata in order to achieve an economic balance between the plant's carbon needs and water use. Here, we present a quantitative theoretical framework to predict allometric relationships between morphological stomatal traits in relation to leaf gas exchange and the required allocation of epidermal area to stomata.
- Our theoretical framework was derived from first principles of diffusion and geometry based on the hypothesis that selection for higher anatomical maximum stomatal conductance (g_{smax}) involves a trade-off to minimize the fraction of the epidermis that is allocated to stomata. Predicted allometric relationships between stomatal traits were tested with a comprehensive compilation of published and unpublished data on 1057 species from all major clades.
- In support of our theoretical framework, stomatal traits of this phylogenetically diverse sample reflect spatially optimal allometry that minimizes investment in the allocation of epidermal area when plants evolve towards higher g_{smax}.
- Our results specifically highlight that the stomatal morphology of angiosperms evolved along spatially optimal allometric relationships. We propose that the resulting wide range of viable stomatal trait combinations equips angiosperms with developmental and evolutionary flexibility in leaf gas exchange unrivalled by gymnosperms and pteridophytes.

Introduction

The colonization of land by terrestrial plants was enabled by the evolution of specialized pores (stomata) on the leaf epidermis that regulate the exchange of water vapour and CO_2 between the leaf interior and the atmosphere (Kenrick & Crane, 1997). Crucially, stomata solved the functional dilemma of facilitating CO_2 diffusion into the leaf for photosynthesis while also limiting the outward diffusion of water vapour (Nobel, 1999). However, this innovation came with one large constraint: the fraction of the epidermis that is allocated to stomata critically determines the benefit they offer. To function properly stomata need to be adequately spaced (Franks & Farquhar, 2007), but to facilitate the highest rates of leaf gas exchange the stomata also need to be present in sufficiently high numbers on the leaf surface (Parlange & Waggoner, 1970). Therefore, both insufficient and excessive investment in stomata incur disadvantages that ultimately influence plant productivity, competition and survival (Vatén & Bergmann, 2012). Despite this fundamental importance, a general theory to explain how plants allocate leaf epidermal area to stomata is lacking. Here, we propose a quantitative theoretical framework to describe the allocation of leaf epidermal area to stomata based on the allometric relationship between morphological stomatal traits and the resulting gas exchange capacity of the epidermis.

The basic morphology of stomata consists of two guard cells that regulate the aperture of a central diffusion pore. A graphical representation of the morphological stomatal traits considered in this study is shown in Fig. 1(a). Stomata may occur on both the upper and lower leaf surface (amphistomaty), or on one leaf surface, which is typically the lower surface (hypostomaty). With the formation of each leaf, the average fraction of the leaf epidermis that is allocated to stomata (f_{gc}) is determined by the average size of the guard cell pair (a_{gc}) and average stomatal density (D_s) (Fig. 1b). Together with the size of the stomatal pore at its anatomical maximum aperture (a_{max}), these traits determine the anatomical maximum stomatal conductance (g_{smax}) of the leaf epidermis. Plants regulate leaf gas exchange dynamically by adjusting stomatal conductance (g_s) over a range between near-zero and g_{smax} by opening and closing the stomatal pore at a time scale of minutes to hours (Farquhar & Sharkey, 1982). These aperture changes may occur through a combination of (passive) responses to leaf water status or (active) responses to abscisic acid

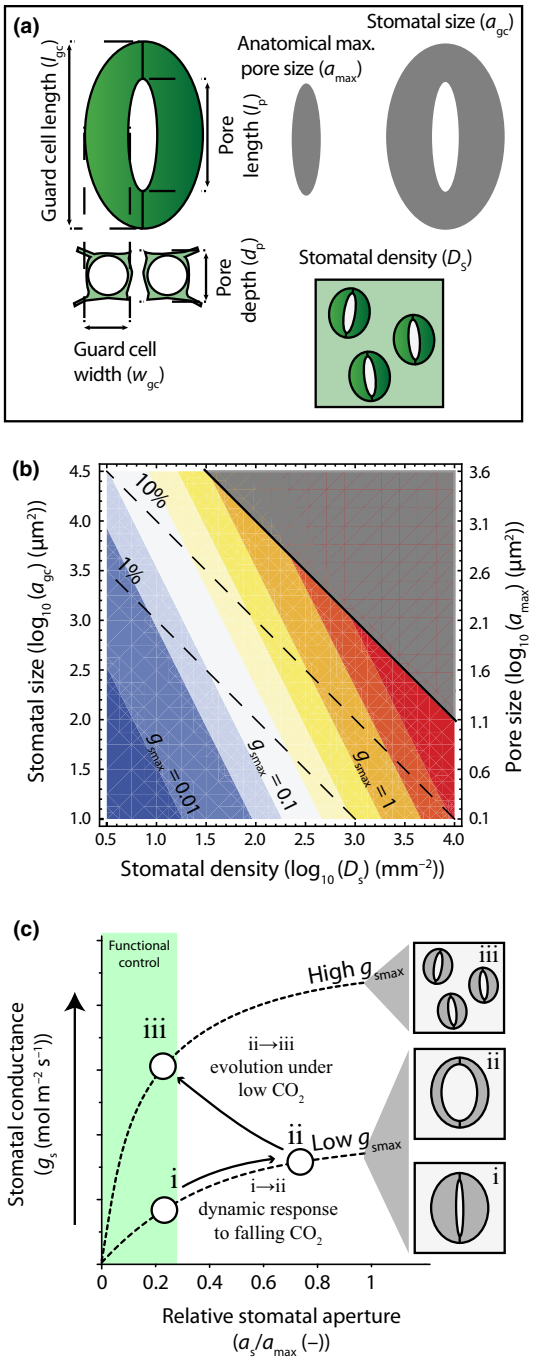

Fig. 1 Theoretical relationships between morphological stomatal traits and leaf gas exchange. (a) Schematized stomatal morphology following Lawson *et al.* (1998) and the specific stomatal traits considered in this study. Stomatal size (a_{gc}) and anatomical maximum pore size (a_{max}) are indicated with grey shapes. (b) Theoretical relationship between the leaf epidermal area fraction allocated to stomata (f_{gc}) (dashed lines and expressed as %) and the anatomical maximum stomatal conductance (g_{smax}) (shaded colours and expressed as mol m^{-2} s^{-1}). The f_{gc} is expressed as a function of $\log_{10}$-transformed values of stomatal density (D_s) and a_{gc}, whereas g_{smax} is expressed as a function of $\log_{10}$-transformed values of D_s and a_{max} (plotted on the 2nd *y*-axis). A constant ratio between a_{max} and a_{gc} of 0.12 (Franks & Beerling, 2009) is assumed for plotting, although this ratio may change depending on stomatal morphology (Franks *et al.*, 2014). (c) Schematic response of stomatal conductance (g_s) to a short-term decrease in atmospheric CO_2 (Farquhar & Sharkey, 1982) before a long-term decrease in atmospheric CO_2 (i → ii), and changes in a_{gc} and D_s during a long-term decrease in atmospheric CO_2 concentration (Franks & Beerling, 2009) that restore functional control on g_s by increasing g_{smax} (Franks *et al.*, 2012b) (ii → iii). The relative stomatal aperture is indicated by the ratio of stomatal aperture (∂_s) to ∂_{max}. The green area denotes the region where guard cells have most functional control on g_s.

(McAdam & Brodribb, 2012, 2014). Although g_s can attain values near g_{smax} under laboratory conditions with low CO_2 and high humidity (Dow *et al.*, 2014), the operational stomatal conductance is relatively constant around a ratio $g_s : g_{smax}$ of 0.2–0.25 under typical growth conditions (McElwain *et al.*, 2015). This ratio corresponds to the region where changes in guard cell turgor pressure have most effective control on stomatal aperture (Franks *et al.*, 2012b). Adjustment of g_{smax} under sustained environmental pressure may therefore confer a functional advantage because it allows more efficient dynamic control on leaf gas exchange under typical growth conditions. The clearest example of this adaptation is that plants respond to prolonged CO_2 changes by adjusting g_{smax} via changes in stomatal densities (Woodward, 1987) and sizes (Franks & Beerling, 2009) in line with a short-term (dynamic) response to CO_2 (Franks *et al.*, 2013) (Fig. 1c). These adaptations may occur through evolution (Franks & Beerling, 2009) or phenotypic changes (de Boer *et al.*, 2011; Lammertsma *et al.*, 2011), whereby the latter appear most pronounced in species with limited active stomatal responses to changes in atmospheric CO_2 (Haworth *et al.*, 2013).

Owing to the close relationship between plant productivity, leaf gas exchange and g_{smax} (McElwain *et al.*, 2015), the density and size of stomata on every leaf, including the proportion of leaf surface they occupy, represents a critical investment in the functional economics of the plant. However, the potential for plants to increase g_{smax} is fundamentally constrained by available space on the leaf epidermis that can viably be allocated to stomata. Three mechanisms have been proposed that relate this spatial constraint to plant function. First, too close spacing of neighbouring stomata may hamper effective opening and closing responses because guard cell movements depend partly on the mechanical advantage of the subsidiary cells (Franks & Farquhar, 2007). Second, as stomata are costly in terms of the energy needed for their operation and maintenance (Assmann & Zeiger, 1987), excess stomata may negatively affect the leaf carbon balance. Third, an increase in stomatal density without concurrent size reduction places stomata closer together and leads to increased interference between the diffusion shells of neighbouring stomata (Lehmann & Or, 2015). From this perspective, evolution pressure on stomatal morphology reflects a trade-off between the benefit of increasing leaf gas exchange and the cost associated with increasing the allocation of leaf epidermal area to stomata. Understanding this trade-off remains relevant for acclimation and adaptation of modern plants (Franks *et al.*, 2013) because, although current atmospheric CO_2 levels are relatively low compared with those that have occurred since the Cretaceous (Fletcher *et al.*, 2008), CO_2 levels have increased dramatically in the last century and are expected to increase further this century (van Vuuren *et al.*, 2011).

Despite a long history of research in this field, a quantitative theory to explain the allometric relationships between morphological stomatal traits is still lacking. Here we derive and test a quantitative theoretical framework that predicts two key allometric relationships between morphological stomatal traits. The first relationship entails the scaling between stomatal sizes a_{gc} and stomatal densities D_s. The second entails the scaling between anatomical maximum pore sizes a_{max} and stomatal sizes a_{gc}. These relationships are derived from generic constraints related to the investment of leaf epidermal area to stomata and the resulting g_{smax}. We test the predicted allometric relationships with a comprehensive compilation of published and unpublished data on the stomatal traits of 1057 species from 156 families that include all major clades and reflect a global range of environments. Our empirical analyses are performed at tree levels of detail. First, we analyse allometric relationships between the morphological stomatal traits of a phylogenetically diverse species group. Secondly, we differentiate between the evolutionary distinct groups of pteridophyte, gymnosperm and angiosperm species. Finally, we analyse a selection of amphistomatous species that, by allocating space on both leaf surfaces to stomata, may reflect an exception to the proposed spatial constraint on stomatal size–density combinations.

Description

Theoretical framework

The theoretical framework presented here is developed based on two premises. The first premise is that evolution of stomatal density together with the size of the guard cells and pores principally reflects selection pressure to realize the benefit of increased g_{smax} (Franks & Beerling, 2009; McElwain *et al.*, 2015). The second premise is that there is a cost associated with increasing the fractional stomatal cover of the leaf epidermis (f_{gc}). Hence, f_{gc} is considered a proxy for the combined costs associated with the operation and maintenance of the stomata (Edwards *et al.*, 1976; Assmann & Zeiger, 1987; Franks & Farquhar, 2007). Our hypothesis entails that the evolution of morphological stomatal traits results in an increase in g_{smax} (the benefit) and a simultaneous decrease in f_{gc} (the cost). From our framework we can derive testable predictions by expressing g_{smax} and f_{gc} in terms of (observable) allometric relationships between the stomatal density D_s, the size of the guard cell pair a_{gc} and the anatomical maximum pore size a_{max}.

Here, the f_{gc} was calculated as the product of stomatal density and stomatal size:

$$f_{gc} = D_s \cdot a_{gc} \qquad \text{Eqn 1}$$

The g_{smax} was calculated from the principles of diffusion (Franks & Farquhar, 2001; Franks & Beerling, 2009):

$$g_{smax} = \frac{D_s \cdot a_{max} \frac{d_{H_2O}}{w_v}}{d_p + \frac{\pi}{2}\sqrt{a_{max}/\pi}} \qquad \text{Eqn 2}$$

(d_{H2O}, diffusivity of water vapour in air; w_v, molar volume of air normalized to 25°C; d_p, depth of the stomatal pore.) For our theoretical analyses of g_{smax}, d_p is assumed equal to the cross-sectional diameter, or width of the guard cell (w_{gc}) (Franks & Farquhar, 2007) and retains a constant ratio (r_{wl}) with guard cell length (l_{gc}) so that $r_{wl} = w_{gc}/l_{gc} \approx 0.36$ across species (Supporting Information Fig. S1). This allows us to express pore depth as:

$$d_p = \sqrt{a_{gc} \cdot r_{wl} \cdot \frac{2}{\pi}}.$$

In order to derive testable predictions from our hypothesis, we represent the allometric relationship between sizes of the guard cell pairs and the stomatal density densities as:

$$a_{gc} = b_s \cdot D_s^{\,S} \qquad \text{Eqn 3}$$

(b_s, offset of the scaling relationship; S, scaling exponent.)

The values of g_{smax} and f_{gc} are linked via the allometric relationship between the anatomical maximum pore size and stomatal size:

$$a_{max} = b_p \cdot a_{gc}^{\,P} \qquad \text{Eqn 4}$$

(b_p, offset of the scaling relationship; P, scaling exponent.)

By inserting the allometric relationships between a_{gc} and D_s (Eqn 3) and between a_{max} and a_{gc} (Eqn 4) into Eqns 1 and 2 we develop a mathematical cost–benefit expression of how g_{smax} changes relative to f_{gc} depending on combined changes in stomatal morphology and stomatal density (see Eqns 8–13 in Methods S1 and Notes S1 for details). This expression quantifies the change in g_{smax} resulting from changes in stomatal density and associated changes in stomatal morphology ($\partial g_{smax}/\partial D_s$), relative to the corresponding change in f_{gc} ($\partial f_{gc}/\partial D_s$), which we term the marginal ratio Λ:

$$\Lambda = \frac{\partial g_{smax}/\partial D_s}{\partial f_{gc}/\partial D_s} \qquad \text{Eqn 5}$$

The full mathematical expression of Λ is difficult to interpret on its own and depends on the allometric relationships given by Eqns 3 and 4, principally the exponents S and P. Hence, we explored a range of realistic values for these exponents to characterize the behaviour of Eqn 5. This behaviour is characterized by the sign of Λ that allows us to recognize three regions which reflect different combinations of increasing/decreasing f_{gc} (cost) and g_{smax} (benefit) as a function of the exponents S and P (Fig. 2a). Based on this behaviour of Eqn 5, our framework yields two testable predictions. The first prediction requires that f_{gc} (the cost) should not increase when D_s increases. This prediction sets the upper bound on the exponent $S \leq -1$, which is valid for region (I) and region (II) in Fig. 2(a). In these regions, the increase in D_s is tied to a decrease in a_{gc} in such a way that f_{gc} (calculated as $D_s \cdot a_{gc}$, cf. Eqn 1) remains constant or decreases.

New Phytologist

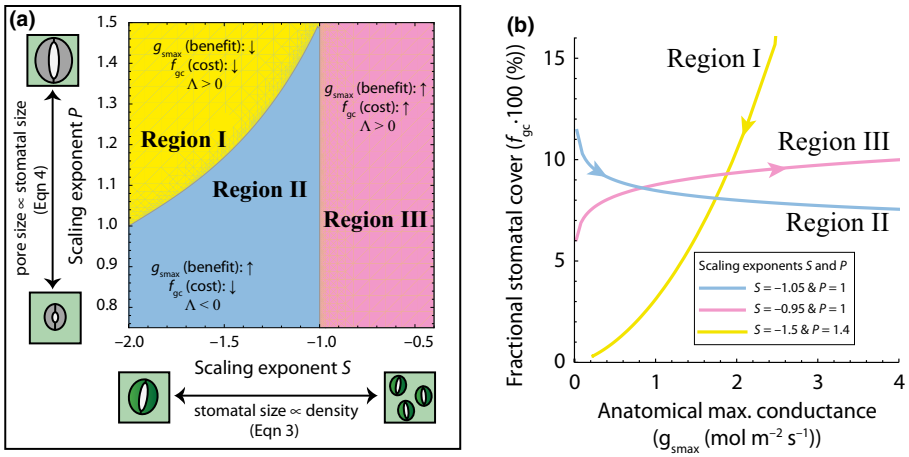

Fig. 2 Theoretical framework on optimal allocation of leaf epidermal area for gas exchange. (a) Sign of the marginal ratio Λ (Eqn 5), which represents the marginal change in g_{smax} under a change in stomatal density ($\partial g_{smax}/\partial D_s$), relative to the corresponding marginal change in f_{gc} ($\partial f_{gc}/\partial D_s$), as a function of the exponents *S* and *P* in the allometric relationships between D_s and a_{gc} (Eqn 3), and between a_{gc} and a_{max} (Eqn 4), respectively. In regions (I) and (III), an increase in D_s leads to same-signed changes of g_{smax} and f_{gc} (Λ > 0), whereas in region (II) an increase in g_{smax} is tied to a decrease in f_{gc} (Λ < 0). (b) Relationships between g_{smax} and f_{gc} depending on the scaling exponents *S* and *P*. The three lines correspond to the regions in (a). Arrows indicate the direction of change resulting from an increase in D_s.

The second prediction requires g_{smax} (the benefit) to increase when D_s increases. This occurs when combinations of scaling exponents *S* and *P* fall in regions (II) and (III) in Fig. 2(a). To satisfy both predictions, which yields Λ < 0, the combination of exponents *S* and *P* should therefore fall in region (II) in Fig. 2(a). Only this specific combination of exponents *S* and *P* results in an increase in g_{smax} and simultaneous decrease in f_{gc} (Fig. 2b). Our physiological interpretation of this situation is that the benefit of increasing g_{smax} is combined with a reduction in the cost associated with f_{gc}.

Data acquisition

In order to test our hypothesis, we compiled previously published and unpublished data on morphological stomatal traits of 1057 species from 156 families that include all major clades and reflect a wide range of environments. We searched the literature by querying the search engines of Scopus and Google scholar with the following search terms: 'stomatal sizes', 'stomatal densities', 'guard cell dimensions', 'stomatal size', 'pore size', 'stomatal morphology' and 'cuticle morphology'. We specifically selected studies that included multiple measurements from single species, multiple species from a single family or multiple species from a single environment. References to the 50 studies included in the compiled dataset are presented in Table S1. From the selected studies we extracted data on stomatal density D_s in combination with the size of the guard cell pair a_{gc}, guard cell length l_{gc}, guard cell width w_{gc}, stomatal pore length (l_p) and pore depth d_p. Typically, stomatal density was reported in literature for the abaxial (lower) leaf side assuming that the leaves are hypostomatous. In those situations, we reported stomatal density as an average density on the abaxial epidermis only. If stomatal density was provided for both leaf sides (with a stomatal ratio > 0.05) the species was flagged as being amphistomatous. To facilitate comparison with hypostomatous species and warrant consistency across all data, the stomatal densities of amphistomatous species reported here reflect the average density on the abaxial and adaxial epidermises. If the size of the guard cell pair a_{gc} was reported without reference to the guard cell dimensions l_{gc} and w_{gc}, we used the reported value. Otherwise, the size of the guard cell pair was calculated as:

$$a_{gc} = \frac{\pi}{2} \cdot l_{gc} \cdot w_{gc} \qquad \text{Eqn 6}$$

The pore size at its anatomical maximum aperture a_{max} was calculated from the reported pore length as:

$$a_{max} = \frac{\pi}{4} f_{lw} \cdot l_p^{\,2} \qquad \text{Eqn 7}$$

(f_{lw}, area fraction of a circle with diameter l_p that is occupied by a_{max}). For f_{lw} we differentiated the basic stomatal morphologies following Franks *et al.* (2014), where f_{lw} ranges between 0.4 and 1 (Table S2). For the species *Oplismenus hirtellus*, *Populus gileadensis* and *Tilia americana* we found $a_{max} > a_{gc}$, which we deemed unrealistic. Owing to the relatively large uncertainty in measuring the length of the stomatal pore (Lawson *et al.*, 1998) we excluded these values of a_{max} from our analyses. We note that this did not significantly alter the observed allometric relationships.

In addition to the published data, we included unpublished measurements of the stomatal traits of 43 species (Tables S1, S3). These measurements were taken by separating the cuticle through maceration of leaf fragments in 5–10% sodium hypochlorite (NaClO). The removed cuticle was dyed with safranin, and mounted in glycerine jelly on glass slides. Cuticles were analysed using optical microscopes and analysis software. Stomatal densities were determined by counting the number of stomata in a minimum of 10 fields of view per leaf. Stomatal dimensions were measured on a minimum of 10 stomata on each leaf.

Data analyses and statistics

Species names as originally reported in the published literature were updated to the latest convention through the Taxonomic Name Resolution Service (Boyle *et al.*, 2013). When multiple observations from a single species were available we used the arithmetic mean to calculate a species average trait value. If multiple averages for a single species were available from different sources, the grand mean was used as the species average. A compilation of all species averaged data on D_s, a_{gc} and a_{max} is provided in Table S3.

We constructed a phylogenetic tree of the taxa included in our dataset with the PHYLOCOM v.4.2 software (Webb *et al.*, 2008) by using the APG III-derived megatree R20120829 (Stevens, 2012). The nodes of the resulting phylogenetic tree were dated using the BLADJ function of PHYLOCOM based on the dating of Wikström *et al.* (2001). The phylogeny of all species included in the compiled dataset is shown in Fig. S2. Based on this phylogeny we calculated the phylogenetically independent contrasts (PICs) (Felsenstein, 1985) of the traits considered using the R package PHYTOOLS (Revell, 2012). Branch lengths were transformed logarithmically to remove any relationship with the standardized contrasts. The phylogenetic signal in each trait was assessed with Blomberg *et al.*'s K (Blomberg *et al.*, 2003) and Pagel's Lambda (Pagel, 1999) using the 'phylosig' function of the R package PHYTOOLS (Revell, 2012).

Our empirical analyses were performed at three levels of detail. First, we analysed the allometric relationships between the morphological stomatal traits of all species present in the compiled dataset. Second, we analysed evolutionarily distinct groups of pteridophyte, gymnosperm and angiosperm species in isolation. Third, we analysed selections of amphistomatous monocot and dicot species in isolation. The allometric relationships presented in this study were obtained by fitting a standardized major axis (SMA) regression on $\log_{10}$-transformed values of species average traits using the R package SMATR-3 (Warton *et al.*, 2012). The SMAs fitted on species average traits data included an offset if the offset was significantly different from 0, whereas the SMAs fitted on the PICs were forced through the origin (Garland *et al.*, 1992). SMA fits were considered valid when the Pearson product–moment correlation coefficient (r) between $\log_{10}$-transformed traits values was significant ($P < 0.05$).

The first prediction of our theoretical framework (e.g. exponent $S \leq -1$) was tested based on 95% confidence intervals (CIs) around the SMA regression slope of the allometric relationship between stomatal size and density (Eqn 3). To test the second prediction (e.g. $\Lambda < 0$) we first derived a mathematical expression for Λ in terms of Eqns 3 and 4 using the Wolfram MATHEMATICA software (see Eqn 5 and Methods S1). The marginal ratio Λ was subsequently calculated from the offsets and exponents found for the allometric relationships as described by Eqns 3 and 4. Uncertainty ranges of Λ were obtained by bootstrapping the (paired) offsets and exponents of the scaling relationships given by Eqns 3 and 4 through resampling the raw data 10 000 times. The prediction that $\Lambda < 0$ was subsequently tested based on the 95% CIs of the (bootstrapped) distributions of Λ.

Differences between group means of g_{smax}, f_{gc} and a_{gc} were tested with a two-sided ANOVA. Post-hoc tests were done with two-sided Student's t-test assuming unequal sample sizes and variances and included a Bonferroni-correction considering that three t-tests are performed after each ANOVA. Values of g_{smax} were square-root transformed prior testing, whereas values of f_{gc} and a_{gc} were $\log_{10}$-transformed.

Results

Allometry in stomatal traits

We tested our hypothesis and the underlying theoretical framework with observations of stomatal traits drawn from a phylogenetically diverse compilation of published and unpublished data of 1057 species in 156 families from a global range of environments (Tables S1, S3). These data reveal the well-known inverse relationship between stomatal density D_s and the size of the guard cell pair a_{gc} ($r^2 = 0.43$, $P < 0.001$ for $\log_{10}$-transformed values) (Fig. 3a). The observed exponent S in this allometric relationship (e.g. Eqn 3) is negative across all species in our dataset and within subsets of angiosperm, gymnosperm and pteridophyte species (Table 1). Considering this relationship across all species and across the subsets of angiosperm and gymnosperm species provides support for our first prediction that $S \leq -1$ (see Table 1 for 95% CIs around the exponent S), which allows D_s to increase without increasing f_{gc}. By contrast, the subset of pteridophyte species shows a shallower inverse relationship with $S = -0.58$ with 95% CIs (-0.70, -0.46). The implication is that across the pteridophytes species in our compiled dataset increases in D_s are associated with increases in f_{gc}.

Our results further show an allometric relationship between the size of the guard cell pair a_{gc} and the anatomical maximum pore size a_{max} across all species in the dataset ($P < 0.001$, $r^2 = 0.50$ for $\log_{10}$-transformed values), and within the subset of angiosperm species ($P < 0.001$, $r^2 = 0.58$ for $\log_{10}$-transformed values) (Fig. 3b). The observed exponent P in these relationships (e.g. Eqn 4) cannot be distinguished from shape-preserving unity (see Table 1 for 95% CIs around the exponent P). No significant relationship (correlation $P > 0.05$ for $\log_{10}$-transformed values) was found between these traits considering the subsets of gymnosperm and pteridophyte species in isolation.

In order to control for potential phylogenetic bias in our data we also obtained the allometric relationships between Phylogenetically Independent Contrasts (PICs) (Felsenstein, 1985) of the traits considered here (Fig. S3). This analysis suggests that the observed relationships are robust to phylogenetic bias (Table S4) despite all traits reflecting phylogenetic signal (Table S5).

Optimal allocation of epidermal area

In order to test whether the combination of observed allometric relationships given by Eqns 3 and 4 supports our second prediction that $\Lambda < 0$ and fall in the region (II) indicated in Fig. 2, we obtained bootstrapped distributions of these relationships considering all species in the compiled dataset and considering subsets

Table 1 Allometric relationships between morphological stomatal traits

Species selection	X variable	Y variable	Sample size	Offset	Median offset	Lower 95% CI offset	Upper 95% CI offset	Exponent	Median exponent	Lower 95% CI exponent	Upper 95% CI exponent	r^2	P
All species	D_s	a_{gc}	1032	b_s	0.10	0.04	0.25	S	−1.03	−1.07	−0.98	0.43	***
Angiosperms	D_s	a_{gc}	927	b_s	0.17	0.06	0.47	S	−1.05	−1.11	−1.00	0.37	***
Gymnosperms	D_s	a_{gc}	38	b_s	12	0.02	8.4×10^{3}	S	−1.25	−1.60	−0.90	0.31	***
Pteridophytes	D_s	a_{gc}	67	b_s	3.0×10^{-5}	3.9×10^{-6}	2.3×10^{-4}	S	−0.58	−0.70	−0.46	0.36	***
Amphistomatous dicot	D_s	a_{gc}	72	b_s	2.1×10^{-4}	2.4×10^{-5}	1.7×10^{-3}	S	−0.70	−0.81	−0.58	0.53	***
Amphistomatous monocot	D_s	a_{gc}	40	b_s	67.00	0.21	2.1×10^{4}	S	−1.43	−1.75	−1.13	0.56	***
All species	a_{gc}	a_{max}	251	b_p	0.05	0.01	0.29	P	0.92	0.84	1.01	0.50	***
Angiosperms	a_{gc}	a_{max}	214	b_p	0.05	0.01	0.31	P	0.92	0.84	1.00	0.58	***
Gymnosperms	a_{gc}	a_{max}	23	b_p	–	–	–	P	–	–	–	–	ns
Pteridophytes	a_{gc}	a_{max}	14	b_p	–	–	–	P	–	–	–	–	ns
Amphistomatous dicot	a_{gc}	a_{max}	19	b_p	5.0×10^{5}	3.8×10^{3}	6.5×10^{7}	P	1.68	1.45	1.91	0.93	***
Amphistomatous monocot	a_{gc}	a_{max}	10	b_p	1.17	9.7×10^{-6}	1.5×10^{5}	P	1.07	0.51	1.63	0.59	**

Offsets and exponents reflect standardized major axis regressions calculated on the species average trait data expressed in the following units: stomatal density (D_s, no. stomata·mm^{-2}), average size of the guard cell pair (a_{gc}, m^2), anatomical maximum aperture (a_{max}, m^2). The r^2 denotes the Pearson product–moment correlation coefficient between $\log_{10}$-transformed traits values. Significance levels of correlation are indicated: ***, $P < 0.001$; **, $P < 0.01$; ns, $P \geq 0.05$.

of angiosperm, gymnosperm and pteridophyte species in isolation. Combinations of the observed exponents S and P and the resulting consequence for the trade-off between changes in g_{smax} and f_{gc} are shown in Fig. 3(c). In support of our hypothesis, we observed that $\Lambda < 0$ across all species and across the subset of angiosperm species (Fig. 3d). As we found no significant scaling relationship between the size of the guard cell pair a_{gc} and the anatomical maximum pore size a_{max} across the subsets of gymnosperm and pteridophyte species, we principally rejected our hypothesis considering these clades in isolation. However, the lack of a significant relationship between a_{max} and a_{gc} in the gymnosperm and pteridophyte clades could be related to the relatively small sample size (Table 1). Hence, we calculated Λ for the subsets of gymnosperm and pteridophyte species assuming that the generic scaling relationship between a_{max} and a_{gc} applies to these clades in isolation. For the subset of pteridophyte species we then observed a marginal ratio $\Lambda > 0$, whereas for gymnosperms the median value of Λ was negative but, considering a 95% confidence limit, this result is statistically not significant (Fig. 3d).

The proposed theoretical framework implies that spatially optimal stomatal scaling requires coordinated evolution of stomatal densities and stomatal morphology in relation to evolution towards higher g_{smax}. This inference is supported by increases in g_{smax} between consecutive evolutionary groups that are not associated with changes in f_{gc} owing to concurrent reductions in the size of the guard cell pair a_{gc} (Fig. 4a). Further support for this inference is found in the inverse relationship between species averages of g_{smax} and stomatal size considering all species together, and within the subsets of angiosperms and gymnosperms (Figs 4b, S3c). We note that these results do not imply that species with small stomata necessarily have high g_{smax}. Rather, smaller stomata extend the upper range of g_{smax} that can viably be obtained within the constraints set by f_{gc} without necessarily limiting the potential to develop leaves with low g_{smax}.

Amphistomaty

Amphistomatous leaves provide an example were the proposed spatial constraint on stomatal size-density combinations may be less pressing owing to the doubling of available epidermal space compared with hypostomatous leaves. Relaxing the spatial constraint on stomatal size-density combinations theoretically allows for the slope S in the allometric relationship between D_s and a_{gc} to be shallower than the area-preserving value of −1. It may therefore be expected that stomatal scaling relationships for amphistomatous angiosperm species result in $\Lambda > 0$ and fall in the region (III) of Fig. 2.

As the subset of all angiosperm species reflects the proposed optimal scaling of stomatal traits, we examined whether a subset of amphistomatous angiosperms deviates from this spatially optimal pattern. The amphistomatous angiosperm species selection consists of dicots and monocots (mostly grasses) which are phylogenetically distinct clades and have distinct leaf morphologies. We therefore analysed the allometric relationships for these

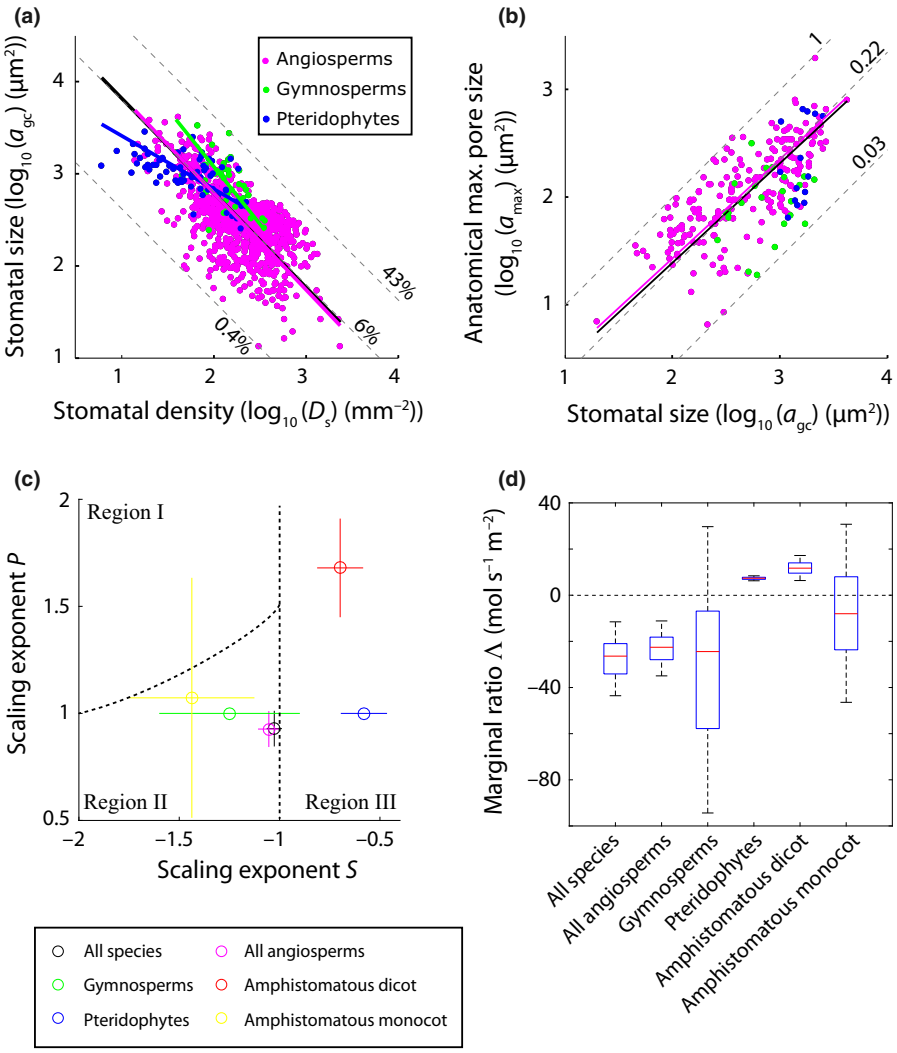

Fig. 3 Allometric relationships between morphological stomatal traits. (a) Log_{10}-transformed values of D_s and a_{gc} and (b) a_{gc} and a_{max}. The solid black lines represent standardized major axis (SMA) regressions fitted on all species; the pink, green and blue lines denote the SMAs across subsets of angiosperm, gymnosperm and pteridophyte species, respectively. See Table 1 for detailed statistics. Maximum, median and minimum values of f_{gc} (expressed as %), and the ratio $a_{max} : a_{gc}$ are indicated by the dashed lines in (a) and (b), respectively. (c) Bootstrapped distributions of the scaling exponents S and P (Eqns 3 and 4, respectively) calculated across the distinct species subsets indicated by the differently coloured symbols. Confidence intervals indicate the 5th and 95th percentiles of the bootstrapped exponents. Dashed lines indicate the borders between the different scaling regions indicated in Fig. 2. (d) Distributions of the bootstrapped values of Λ considering all species present in the compiled dataset and distinct species subsets. The red line inside boxes indicates the median of the bootstrapped distribution, the bottom and top of each box denotes the first and third quartile, respectively, whiskers denote the 5th and 95th percentiles.

groups separately. In line with a relaxation of the spatial constraint, the subgroup of amphistomatous dicots shows allometric relationships with $\Lambda > 0$ (Fig. 3c,d) that fall in the region (III) of Fig. 2, specifically because the exponent $S > -1$ (Fig. S4). Hence, increases in g_{smax} are tied to increases in f_{gc} across this group of species. By contrast, we found that $S < -1$ for the subset of amphistomatous monocots. As a result, the median of the bootstrapped allometric relationships for amphistomatous monocots results in $\Lambda < 0$ and falls in region (II) of Fig. 2, with the 95% CIs overlapping with region (I), owing to the relatively large spread in the observed exponent P.

Discussion

Our theoretical framework and empirical analyses suggest that the evolution of morphological stomatal traits involves a trade-off to maximize the gas exchange capacity of the epidermis while minimizing the fraction of the epidermis that is covered by stomata. This result is in line with fossil evidence (Franks & Beerling, 2009) which suggests that evolutionary increases in g_{smax} were closely related to increases in stomatal densities and decreases in stomatal (pore) size (Assouline & Or, 2013), especially by evolution within the angiosperm clade (de Boer *et al.*, 2012). These stomatal size–density relationships may have evolved because variations in stomatal density are controlled by cell-to-cell signalling mechanisms that regulate spacing between stomata (Lee *et al.*, 2015) as well as phenotypic adjustments to environmental conditions (Bergmann & Sack, 2007; Doheny-Adams *et al.*, 2012). Stomatal size is less plastic than stomatal density (Zhang *et al.*, 2012) owing to its relationship with genome size (Beaulieu *et al.*, 2008; Franks *et al.*, 2012a). Still, the association between genome size and stomatal size may change slightly under environmental pressure (Lomax *et al.*, 2009; Jordan *et al.*, 2015) and thereby facilitate adaptive evolution of stomatal (pore) size in coordination with changes in stomatal density. Smaller stomata may also allow for faster dynamic responses in stomatal aperture (Drake *et al.*, 2013), a benefit that may specifically confer gas exchange advantage to angiosperms owing to their accurate control on stomatal aperture (Brodribb *et al.*, 2009; McAdam & Brodribb, 2012, 2014).

Our results provide no support for spatially optimal co-evolution of stomatal traits occurring within the pteridophyte

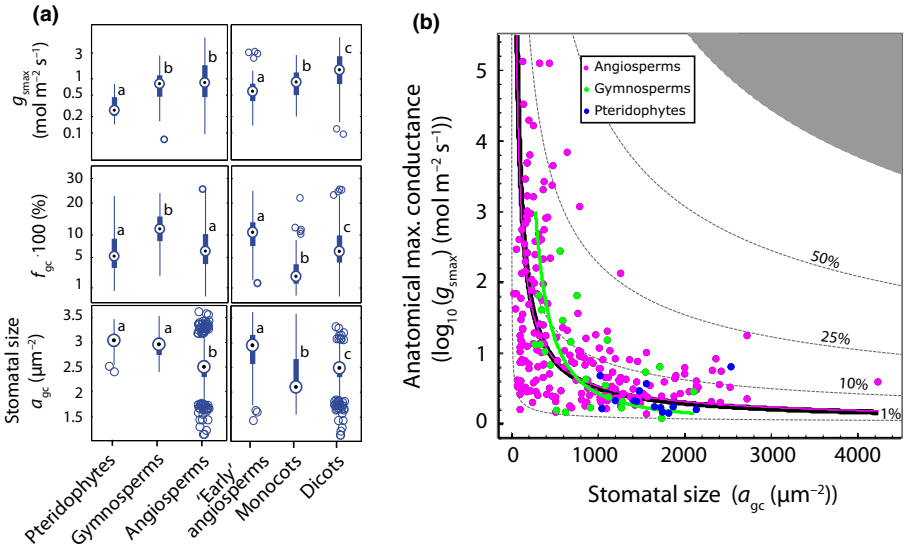

Fig. 4 Reduction of stomatal size extends viable ranges in g_{smax}. (a) Box plots of g_{smax} (upper panels), f_{gc} (middle panels) and a_{gc} (lower panels) separated for pteridophytes, gymnosperms and angiosperms (left) and three angiosperm subclades (right). The early angiosperm clade includes the ANITA-grade, Chloranthales and magnoliids. Circles in boxes indicate the median, the bottom and top of each box denotes the first and third quartile, respectively, and whiskers denote the 5th and 95th percentiles. Data points outside whiskers are shown individually. Letters denote significant differences between group means ($P < 0.05$, with Bonferroni correction). (b) Two-dimensional morphospace expressed in terms of a_{gc} and g_{smax}. Data points indicate species-averaged combinations a_{gc} and g_{smax}, with g_{smax} calculated following Eqn 1. The solid black line represent the standardized major axis (SMA) regressions fitted on all species, the pink and green lines denote the SMAs across subsets of angiosperm and gymnosperm species, respectively. See Table 1 and Supporting Information Table S4 for detailed statistics. Dashed lines indicate f_{gc} as a percentage.

and gymnosperm clades. The lack of clear stomatal scaling relationships within these clades could be related to the relatively small sample size in relation to their relatively narrow ranges in stomatal size–density combinations. In contrast to angiosperms that occupy a wide morphospace in terms of stomatal size–density combinations, pteridophytes and gymnosperms are restricted to combinations of relatively few and large stomata. These narrow morphological ranges could reflect limited selection pressure on stomatal morphology in relation to g_{smax}. In contrast to angiosperms, the leaf gas exchange capacity of gymnosperm and pteridophyte leaves is restricted by their relatively low leaf water transport capacity (Brodribb *et al.*, 2005). Owing to the close relationships between leaf water transport capacity and stomatal gas exchange (Sack & Scoffoni, 2013) species from these clades may experience little competitive advantage from increasing g_{smax} by adjusting stomatal morphology because the leaf water transport capacity is not sufficient to keep the stomata open under typical growth conditions (McElwain *et al.*, 2015).

Yet, the success of species with relatively large stomata suggests that this morphology, despite incurring potential functional limitations, does not threaten their survival. However, it might be reflective of adaptation to specific environmental niches. The angiosperm family Liliaceae, for example, contains a relatively large proportion of species with large stomata but these are restricted predominantly to regions with low spring temperatures (Leitch *et al.*, 2007). Similarly, the persistence of large stomata in the pteridophyte clade hints at limited selection for high g_{smax} owing to their relatively low leaf water transport capacity and predominant occurrence in low-light environments (Brodribb *et al.*, 2005, 2007). The large stomata in the gymnosperm clade could be associated with their relatively low leaf water transport capacity (Brodribb *et al.*, 2005, 2007) in relation to environments that select for leaf longevity rather than high productivity (Bond, 1989; Reich *et al.*, 2014). A similar mechanism could be invoked to explain the difference in stomatal scaling relationships between the subgroups of amphistomatous dicots and monocots. Monocots have, on average, sturdier leaves with longer life spans (Onoda *et al.*, 2011) and distinctly lower leaf vein densities than other angiosperm subclades (Roddy *et al.*, 2013). As a result, monocots may experience little evolution pressure to increase leaf gas exchange capacity despite having both leaf sides available to allocate to stomata. Hence, the competitive advantage of spatially optimal allocation of leaf epidermal area to stomata could be negated by specific growth conditions in relation to leaf hydraulics and leaf morphology.

Our results highlight that the stomatal morphology of angiosperms evolved towards higher g_{smax} along spatially optimal allometric relationships. As a result, this clade now occupies a specific part of the morphospace that is associated with smallest stomata. Angiosperms thereby extend the upper range of g_{smax} beyond those of gymnosperms and pteridophytes without limiting the possibility to develop leaves with low g_{smax} by downregulating stomatal density. The resulting wide range of viable g_s–g_{smax} combinations equips angiosperms with developmental and evolutionary flexibility in leaf gas exchange (McElwain *et al.*, 2015) that, in combination with innovations of leaf water transport tissue (Feild *et al.*, 2011; de Boer *et al.*, 2012), enables them to thrive in diverse and ever-changing global climates.

Acknowledgements

This research was funded with an Australia Awards Endeavour research fellowship and a NWO VENI research grand. We kindly thank Jennifer McElwain and the anonymous reviewers for their comments and suggestions.

Author contributions

H.J.B., C.A.P. and E.J.V. designed the research. H.J.B., S.C.D., P.J.F. and C.A.P. analysed data, H.J.B., P.J.F., E.J.V. and F.W-C. contributed data. H.J.B. wrote the manuscript. All authors discussed the results and commented on the manuscript.

References

Assmann SM, Zeiger E. 1987. Guard cell bioenergetics. In: Zeiger E, Farquhar G, Cowan I, eds. *Stomatal function*. Palo Alto, CA, USA: Stanford University Press, 163–193.

Assouline S, Or D. 2013. Plant water use efficiency over geological time – evolution of leaf stomata configurations affecting plant gas exchange. *PLoS ONE* **8**: e67757.

Beaulieu JM, Leitch IJ, Patel S, Pendharkar A, Knight CA. 2008. Genome size is a strong predictor of cell size and stomatal density in angiosperms. *New Phytologist* **179**: 975–986.

Bergmann DC, Sack FD. 2007. Stomatal development. *Annual Review of Plant Biology* **58**: 163–181.

Blomberg SP, Garland T, Ives AR. 2003. Testing for phylogenetic signal in comparative data: behavioral traits are more labile. *Evolution* **57**: 717–745.

de Boer HJ, Eppinga MB, Wassen MJ, Dekker SC. 2012. A critical transition in leaf evolution facilitated the Cretaceous angiosperm revolution. *Nature Communications* **3**: 1221.

de Boer HJ, Lammertsma EI, Wagner-Cremer F, Dilcher DL, Wassen MJ, Dekker SC. 2011. Climate forcing due to optimization of maximal leaf conductance in subtropical vegetation under rising CO_2. *Proceedings of the National Academy of Sciences, USA* **108**: 4041–4046.

Bond WJ. 1989. The tortoise and the hare: ecology of angiosperm dominance and gymnosperm persistence. *Biological Journal of the Linnean Society* **36**: 227–249.

Boyle B, Hopkins N, Lu Z, Raygoza Garay JA, Mozzherin D, Rees T, Matasci N, Narro ML, Piel WH, Mckay SJ *et al.* 2013. The taxonomic name resolution service: an online tool for automated standardization of plant names. *BMC Bioinformatics* **14**: 16.

Brodribb TJ, Feild TS, Jordan GJ. 2007. Leaf maximum photosynthetic rate and venation are linked by hydraulics. *Plant Physiology* **144**: 1890–1898.

Brodribb TJ, Holbrook NM, Zwieniecki MA, Palma B. 2005. Leaf hydraulic capacity in ferns, conifers and angiosperms: impacts on photosynthetic maxima. *New Phytologist* **165**: 839–846.

Brodribb TJ, McAdam SAM, Jordan GJ, Feild TS. 2009. Evolution of stomatal responsiveness to CO_2 and optimization of water-use efficiency among land plants. *New Phytologist* **183**: 839–847.

Doheny-Adams T, Hunt L, Franks PJ, Beerling DJ, Gray JE. 2012. Genetic manipulation of stomatal density influences stomatal size, plant growth and tolerance to restricted water supply across a growth carbon dioxide gradient. *Philosophical Transactions of the Royal Society B* **367**: 547–555.

Dow GJ, Berry JA, Bergmann DC. 2014. The physiological importance of developmental mechanisms that enforce proper stomatal spacing in *Arabidopsis thaliana*. *New Phytologist* **201**: 1205–1217.

Drake PL, Froend RH, Franks PJ. 2013. Smaller, faster stomata: scaling of stomatal size, rate of response, and stomatal conductance. *Journal of Experimental Botany* **64**: 495–505.

Edwards M, Meidner H, Sheriff DW. 1976. Direct measurements of turgor pressure potentials of guard cells. II. The mechanical advantage of subsidiary cells, the Spannungsphase and the optimal leaf water deficit. *Journal of Experimental Botany* **27**: 163–171.

Farquhar GD, Sharkey TD. 1982. Stomatal conductance and photosynthesis. *Annual Review of Plant Physiology* **33**: 317–345.

Feild TS, Brodribb TJ, Iglesias A, Chatelet DS, Baresch A, Upchurch GR, Gomez B, Mohr BAR, Coiffard C, Kvacek J *et al.* 2011. Fossil evidence for Cretaceous escalation in angiosperm leaf vein evolution. *Proceedings of the National Academy of Sciences, USA* **108**: 8363–8366.

Felsenstein J. 1985. Phylogenies and the comparative method. *American Naturalist* **125**: 1–15.

Fletcher BJ, Brentnall SJ, Anderson CW, Berner RA, Beerling DJ. 2008. Atmospheric carbon dioxide linked with Mesozoic and early Cenozoic climate change. *Nature Geoscience* **1**: 43–48.

Franks PJ, Adams MA, Amthor JS, Barbour MM, Berry JA, Ellsworth DS, Farquhar GD, Ghannoum O, Lloyd J, McDowell N *et al.* 2013. Sensitivity of plants to changing atmospheric CO_2 concentration: from the geological past to the next century. *New Phytologist* **197**: 1077–1094.

Franks PJ, Beerling DJ. 2009. Maximum leaf conductance driven by CO_2 effects on stomatal size and density over geologic time. *Proceedings of the National Academy of Sciences, USA* **106**: 10343–10347.

Franks PJ, Farquhar GD. 2001. The effect of exogenous abscisic acid on stomatal development, stomatal mechanics, and leaf gas exchange in *Tradescantia virginiana*. *Plant Physiology* **125**: 935–942.

Franks PJ, Farquhar GD. 2007. The Mechanical diversity of stomata and its significance in gas-exchange control. *Plant Physiology* **143**: 78–87.

Franks PJ, Freckleton RP, Beaulieu JM, Leitch IJ, Beerling DJ. 2012a. Megacycles of atmospheric carbon dioxide concentration correlate with fossil plant genome size. *Philosophical transactions of the Royal Society B* **367**: 556–564.

Franks PJ, Leitch IJ, Ruszala EM, Hetherington AM, Beerling DJ. 2012b. Physiological framework for adaptation of stomata to CO_2 from glacial to future concentrations. *Philosophical Transactions of the Royal Society B* **367**: 537–546.

Franks PJ, Royer DL, Beerling DJ, Van de Water PK, Cantrill DJ, Barbour MM, Berry JA. 2014. New constraints on atmospheric CO_2 concentration for the Phanerozoic. *Geophysical Research Letters* **41**: 2014GL060457.

Garland T, Harvey PH, Ives AR. 1992. Procedures for the analysis of comparative data using phylogenetically independent contrasts. *Systematic Biology* **41**: 18–32.

Haworth M, Elliott-Kingston C, McElwain JC. 2013. Co-ordination of physiological and morphological responses of stomata to elevated [CO_2] in vascular plants. *Oecologia* **171**: 71–82.

Jordan GJ, Carpenter RJ, Koutoulis A, Price A, Brodribb TJ. 2015. Environmental adaptation in stomatal size independent of the effects of genome size. *New Phytologist* **205**: 608–617.

Kenrick P, Crane PR. 1997. The origin and early evolution of plants on land. *Nature* **389**: 33–39.

Lammertsma EI, de Boer HJ, Dekker SC, Dilcher DL, Lotter AF, Wagner-Cremer F. 2011. Global CO_2 rise leads to reduced maximum stomatal conductance in Florida vegetation. *Proceedings of the National Academy of Sciences, USA* **108**: 4035–4040.

Lawson T, James W, Weyers J. 1998. A surrogate measure of stomatal aperture. *Journal of Experimental Botany* **49**: 1397–1403.

Lee JS, Hnilova M, Maes M, Lin Y-CL, Putarjunan A, Han S-K, Avila J, Torii KU. 2015. Competitive binding of antagonistic peptides fine-tunes stomatal patterning. *Nature* **522**: 439–443.

Lehmann P, Or D. 2015. Effects of stomata clustering on leaf gas exchange. *New Phytologist* **207**: 1015–1025.

Leitch IJ, Beaulieu JM, Cheung K, Hanson L, Lysak MA, Fay MF. 2007. Punctuated genome size evolution in Liliaceae. *Journal of Evolutionary Biology* **20**: 2296–2308.

Lomax BH, Woodward FI, Leitch IJ, Knight CA, Lake JA. 2009. Genome size as a predictor of guard cell length in *Arabidopsis thaliana* is independent of environmental conditions. *New Phytologist* **181**: 311–314.

McAdam SAM, Brodribb TJ. 2012. Stomatal innovation and the rise of seed plants. *Ecology Letters* **15**: 1–8.

McAdam SAM, Brodribb TJ. 2014. Separating active and passive influences on stomatal control of transpiration. *Plant Physiology* **164**: 1578–1586.

McElwain JC, Yiotis C, Lawson T. 2015. Using modern plant trait relationships between observed and theoretical maximum stomatal conductance and vein density to examine patterns of plant macroevolution. *New Phytologist* **209**: 94–103.

Nobel PS. 1999. *Physicochemical and environmental plant physiology.* San Diego, CA, USA: Academic Press.

Onoda Y, Westoby M, Adler PB, Choong AMF, Clissold FJ, Cornelissen JHC, Díaz S, Dominy NJ, Elgart A, Enrico L *et al.* 2011. Global patterns of leaf mechanical properties. *Ecology Letters* **14**: 301–312.

Pagel M. 1999. Inferring the historical patterns of biological evolution. *Nature* **401**: 877–884.

Parlange J-Y, Waggoner PE. 1970. Stomatal dimensions and resistance to diffusion. *Plant Physiology* **46**: 337–342.

Reich PB, Rich RL, Lu X, Wang Y-P, Oleksyn J. 2014. Biogeographic variation in evergreen conifer needle longevity and impacts on boreal forest carbon cycle projections. *Proceedings of the National Academy of Sciences, USA* **111**: 13703–13708.

Revell LJ. 2012. phytools: an R package for phylogenetic comparative biology (and other things). *Methods in Ecology and Evolution* **3**: 217–223.

Roddy AB, Guilliams CM, Lilittham T, Farmer J, Wormser V, Pham T, Fine PVA, Feild TS, Dawson TE. 2013. Uncorrelated evolution of leaf and petal venation patterns across the angiosperm phylogeny. *Journal of Experimental Botany* **64**: 4081–4088.

Sack L, Scoffoni C. 2013. Leaf venation: structure, function, development, evolution, ecology and applications in the past, present and future. *New Phytologist* **198**: 983–1000.

Stevens PF. 2012. *Angiosperm Phylogeny website, v.12, July 2012.* [WWW document] URL http://www.mobot.org/MOBOT/research/APweb/. [accessed 2 September 2014].

Vatén A, Bergmann DC. 2012. Mechanisms of stomatal development: an evolutionary view. *EvoDevo* **3**: 11.

van Vuuren DP, Edmonds J, Kainuma M, Riahi K, Thomson A, Hibbard K, Hurtt GC, Kram T, Krey V, Lamarque J-F *et al.* 2011. The representative concentration pathways: an overview. *Climatic Change* **109**: 5–31.

Warton DI, Duursma RA, Falster DS, Taskinen S. 2012. smatr 3 – an R package for estimation and inference about allometric lines. *Methods in Ecology and Evolution* **3**: 257–259.

Webb CO, Ackerly DD, Kembel SW. 2008. Phylocom: software for the analysis of phylogenetic community structure and trait evolution. *Bioinformatics* **24**: 2098–2100.

Wikström N, Savolainen V, Chase MW. 2001. Evolution of the angiosperms: calibrating the family tree. *Proceedings of the Royal Society of London B* **268**: 2211–2220.

Woodward FI. 1987. Stomatal numbers are sensitive to increases in CO_2 from pre-industrial levels. *Nature* **327**: 617–618.

Zhang L, Niu H, Wang S, Zhu X, Luo C, Li Y, Zhao X. 2012. Gene or environment? Species-specific control of stomatal density and length. *Ecology and Evolution* **2**: 1065–1070.

Supporting Information

Additional supporting information may be found in the online version of this article.

Fig. S1 Relationship between guard cell length and width.

Fig. S2 Phylogenetic tree of all species included in the stomatal trait dataset.

Fig. S3 Allometry between independent contrasts.

Fig. S4 Allometric relationships between stomatal traits of amphistomatous monocots and dicots.

Table S1 References to original data sources used in the compiled dataset on species average stomatal traits

Table S2 Geometric constant f_{lw} used for calculating g_{smax} for different stomata types

Table S3 Compilation of species average stomatal trait values

Table S4 Allometric relationships between phylogenetically independent contrasts of the morphological stomatal traits

Table S5 Test for phylogenetic signal in the traits considered based on Blomberg *et al.*'s K and Pagel's λ

Methods S1 Detailed derivation and expression of the marginal ratio Λ.

Notes S1 Script file to be opened with Wolfram Mathematica software containing the derivation and expression of the marginal ratio Λ.

Please note: Wiley Blackwell are not responsible for the content or functionality of any supporting information supplied by the authors. Any queries (other than missing material) should be directed to the *New Phytologist* Central Office.